JAES | JOURNAL OF APPLIED ENGINEERING SCIENCE | www.engineeringscience.rs
ISTRAŽIVANJA I PROJEKTOVANJA ZA PRIVREDU

Indexed by

INFLUENCE OF APPLICATION OF SANDWICH PANEL ON STATIC AND DYNAMIC BEHAVIOUR OF FERRY RO-RO RAMP DOOR

Tuswan Tuswan
Institut Teknologi Sepuluh Nopember, Kampus ITS Sukolilo, Department of Naval Architecture, Surabaya, Indonesia

Achmad Zubaydi
Institut Teknologi Sepuluh Nopember, Kampus ITS Sukolilo, Department of Naval Architecture, Surabaya, Indonesia

Bambang Piscesa
Institut Teknologi Sepuluh Nopember, Kampus ITS Sukolilo, Department of Civil Engineering, Surabaya, Indonesia

Abdi Ismail
Institut Teknologi Sepuluh Nopember, Kampus ITS Sukolilo, Department of Naval Architecture, Surabaya, Indonesia

Rizky Chandra Ariesta
Institut Teknologi Sepuluh Nopember, Kampus ITS Sukolilo, Department of Naval Architecture, Surabaya, Indonesia

Muhammad Fathi Ilham
Institut Teknologi Sepuluh Nopember, Kampus ITS Sukolilo, Department of Naval Architecture, Surabaya, Indonesia

Fikri Indra Mualim
Institut Teknologi Sepuluh Nopember, Kampus ITS Sukolilo, Department of Naval Architecture, Surabaya, Indonesia

Key words: *structural strength, free vibration, debonding, sandwich panel, ramp door, ferry ro-ro*

Cite article:
Tuswan, T., Achmad, Z., Bambang, P., Abdi, I., Rizky, C. A., Muhammad, F. I. & Fikri, I. M. [2021]. Influence of application of sandwich panel on static and dynamic behaviour of ferry ro-ro ramp door. *Journal of Applied Engineering Science*, 19(1) 208 - 216. DOI:10.5937/jaes0-27708

Online aceess *of full paper is available at: www.engineeringscience.rs/browse-issues*

Istraživanja i projektovanja za privredu
Journal of Applied Engineering Science

Original Scientific Paper

doi:10.5937/jaes0-27708

Paper number: 19(2021)1, 783, 208-216

INFLUENCE OF APPLICATION OF SANDWICH PANEL ON STATIC AND DYNAMIC BEHAVIOUR OF FERRY RO-RO RAMP DOOR

Tuswan Tuswan[1], Achmad Zubaydi[1]*, Bambang Piscesa[2], Abdi Ismail[1], Rizky Chandra Ariesta[1], Muhammad Fathi Ilham[1], Fikri Indra Mualim[1]

[1]Institut Teknologi Sepuluh Nopember, Kampus ITS Sukolilo, Department of Naval Architecture, Surabaya, Indonesia

[2]Institut Teknologi Sepuluh Nopember, Kampus ITS Sukolilo, Department of Civil Engineering, Surabaya, Indonesia

The implementation of a sandwich panel on the marine structure needs better knowledge of mechanical behaviour, primarily static and dynamic response. The static and dynamic response is investigated due to the application of a sandwich panel on the ferry ro-ro ramp door using finite element software ABAQUS. Five modification models using different sandwich thickness and stiffener configuration were compared using static analysis to analyze a comparison of structural strength and weight saving. Additionally, the dynamic response was also investigated due to debonding problem. The influence of debonding ratio, geometry, number of debonding, debonding depth, debonding location, and boundary condition was carried out. Debonding was estimated by using free vibration analysis where the Lanczos method for eigen values extraction was applied. Result of the static analysis showed that Model C caused an increase in strength to weight ratio compared to the existing model. Furthermore, the natural frequency was being calculated as modal parameters to investigate the debonding problem. The natural frequency of the debonded model decreased due to discontinuity in the damaged area. The dynamic response using natural frequency change can be performed as a structural health monitoring technique.

Key words: structural strength, free vibration, debonding, sandwich panel, ramp door, ferry ro-ro

INTRODUCTION

The lightweight sandwich structure has been primarily developed in the wide range of application engineering fields, specifically in the shipbuilding industry. The aim of structural design and optimization in the shipbuilding industry is to increase cargo-carrying capability. However, the applications of lightweight sandwich have so far been limited to naval vessels and non-structural components in commercial vessels. In most general cases, the structural design and optimization are assessed either through modifying the existing structural dimension or assembling alternative lightweight material in which the strength to weight ratio is a primary optimization parameter. Several investigations toward the application of sandwich structure on various ship structural components have shown advantages. It increases the strength and weight ratio [1-3], has excellent damping characteristics [4], leads manufacturing the structure less-complex, and simplifies the construction process [5]. An extensive range research study of the application of sandwich structure due to static and dynamic behaviour and weight-saving analysis in the various ship structure was also mentioned, such as in the ship deck [2, 6], car deck [7-9], hull structure [3], and other various structures. The mentioned result explains that the increase of strength to weight ratio varied explicitly relied on the type of applied structural component, sandwich-type and material, and modification technique.

Although the application of the sandwich panel seems easy in manufacturing, the rigidity issues and several damage problems should also be taken into consideration. The face-core interface layer is often the most vulnerable part [10]. The significant differences between the thickness and material properties of constitutive features make it susceptible to debonding [11]. It causes a large deformation between the interface layer and the internal failure in the outer core material [5], which can degrade the integrity of the structure [12]. One of the reasons that caused debonding is the difficulty in controlling the proper bonding during manufacturing [13, 14]. Therefore, a non-destructive structural health monitoring technique (SHM) in the early stage is necessary.

The presence of the debonding can be recognized by finite element modal analysis [11]. The result can be proposed as an initial study to strengthen the efficiency of SHM. This basic principle is to compare the modal parameters between healthy and debonded models using dynamic properties such as natural frequencies [9, 15-19], mode shapes [20], frequency response functions (FRF) [21, 22], and time or frequency domain data [8, 23]. Influence of debonding size, location, and type on the modal parameter was investigated in [15]. Then, a comparison of single and multiple debonding was also evaluated in [16]. The review of debonding modelling with a different type of analysis was mentioned in [11]. All mentioned summaries only analyze debonding in the

*zubaydi@na.its.ac.id

simple structure. So, further study needs to be conducted in a complex structure such as the ramp door of the ferry ro-ro ship structure.

In this paper, the potential implementation of sandwich panels on the ramp door model toward static and dynamic behaviour using ABAQUS software is investigated. A total of five different configuration models based on the configuration of sandwich thickness and stiffener configuration are analyzed using the static analysis to obtain a comparison of structural strength to weight ratio. To gain more observation, the influence over a wide range of debonding ratio, geometry, number of debonding, debonding depth, location, and boundary condition will be analyzed.

MODELLING DESCRIPTION OF APPLICATION OF SANDWICH PANEL

Application of sandwich panel on ramp door model

The reference model used is a ramp door of Ferry Ro-Ro 300 GT. The existing model is entirely constructed by two stiffened steel plates connected by stiffeners. The configuration detail of sandwich panel application is illustrated in Fig. 1. The change was calculated based on DNV-GL rules using strength index criteria to meet the equivalent strength, see in [24]. The dimension of top and bottom stiffened plates of the existing ramp door is 8m in length, 8.6m in width. Five modification models are modelled by varying top and bottom sandwich thickness, eliminating longitudinal and transverse stiffeners, and changing stiffener profile. The sandwich panels use steel material as the faceplate and resin/clamshell as core material. The material properties used in this analysis was noticed in [9]. The proposed model modifications with complete configuration are adequately presented in Table 1.

Weight comparison between existing and modification models is illustrated in Table 1. From the diagram, it can be reviewed that the usage of the sandwich panel considerably decreases the weight of the structure. However, the proposed Model A without changing existing stiffener results in marginally weight increase by about 0.3%. Model B, Model C, and Model D produce the weight-saving about 10.3%, 14.1%, and 21.2%, serially. Moreover, proposed Model E achieves the highest weight saving about 28.3%. Compared with similar research regarding the application of sandwich panel with the same material properties in different ship structure was stated in [2]. It noted that the implementation of a sandwich panel in ferry ro-ro car deck comprehensively reduced the structural deck about 12%. Another research in [7] showed that the weight savings could be obtained in the range of 8.87% - 11.6% in the car deck model. The application of a sandwich panel in the side hull structure was also stated in [3]. The weight saving can be reached up to 17%. However, even though this application offers promising benefits, the weight saving of the hybrid sandwich application more significant than 50% can be rarely found.

Finite element structural strength analysis

Table 1: Model variations due to the application of sandwich on the ramp door

Model	Top thickness (mm)	Bottom thickness (mm)	Longitudinal stiffener	Transverse stiffener	Weight (tons)
Existing	10	12	11 (T profile)	16 (T profile)	22.9
Model A	5-15-5	5-15-5	11	16	23.06
Model B	5-15-3	5-15-3	11	16	20.63
Model C	5-15-3	5-15-3	12	12	19.76
Model D	5-15-3	5-15-3	9	9	18.11
Model E	5-15-3	5-15-3	6	6	16.47

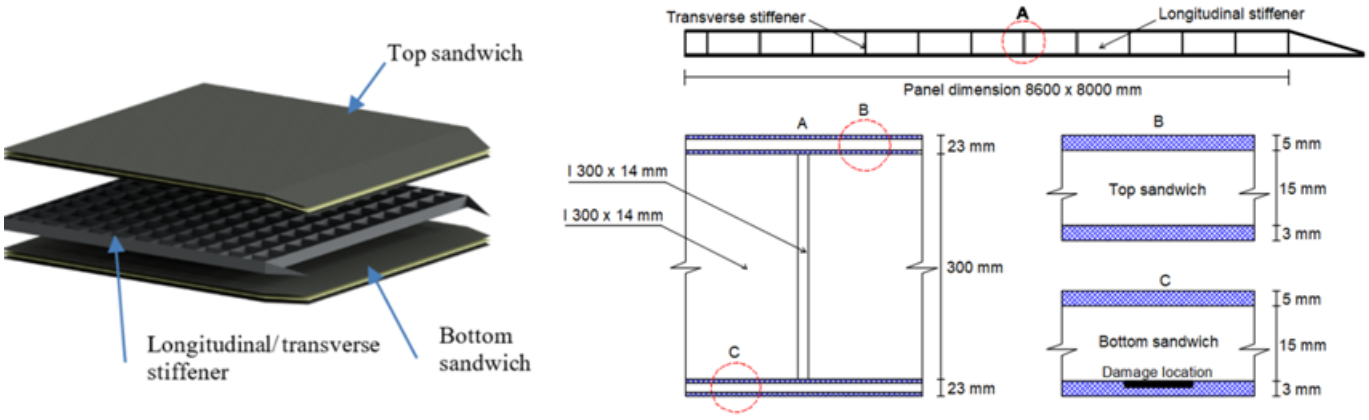

Figure 1: Configuration detail of application of sandwich panel on ramp door

The purpose of the application of the sandwich panel on the ramp door model is to achieve the optimum configuration model, which has the highest strength to weight ratio. In the finite element model discretization of the models, the sandwich panel can be modelled using the layer-wise solid/shell element. Both faceplate and stiffener were modelled using the eight-node quadrilateral shell element (SC8R), and core material was modelled using the eight-node hexahedral element (3D8I). Contact modelling between parts of the structure was modelled by tie constraints. Meanwhile, the boundary condition should be organized in such a way that it could be the same as the real condition. Clamped in the rear and front ramp door and free in the side ramp door (CFCF) was applied.

Design load scenarios for strength calculation was calculated based on DNV-GL [25]. The total static load is the sum of local pressure represented vehicle load and uniformly distributed load from the weight of the ramp door itself. The vehicle load is the sum of chassis weight and the cargo. The vehicle utilizes a single wheel configuration in the front side and double-double axis in the rear side with the same load print (1x0.3m). Both front and rear wheel load are 60kN and 90kN, respectively. The governing equation for the static analysis is shown in Eq. (1), and the mentioned parameters are presented in Eq. (2)

$$\{F\} = [K]\{U\} \quad (1)$$

$$\sigma = P/A \ , \tau = \ F/A \ , \epsilon = \delta/L \quad (2)$$

Where: *{F}* is loads; *[K]* is known (geometry, material properties), *{U}* is displacements; σ is the normal stress; *P* is the force; *A* is the surface area perpendicular to the force; τ is the shear stress; *F* is the force; *A* is the surface area parallel to the force; ϵ is the strain; δ is the deformation; *L* is the length.

Finite element development for free vibration analysis

The free vibration analysis of Model C was performed using a linear perturbation load step where Lanczos method for extracting eigenvalues was applied in the first ten-mode. The finite element discretization and material properties are explained in Section 2.2. Debonding was modelled as artificial damage at the face-core interface layer. The debonding size is defined by a damage parameter ($D_{\%}$) designating the ratio of the debonded area (A_d) to the entire interface layer area of the sandwich (A_{total}). During the pre-processing, debonding is modelled by creating a gap between two constitutive layers. In the present investigation, two different simplified with and without spring contact modelling strategies will be investigated. To prevent the overlapping, a spring contact element modelling is inserted, as depicted in Fig. 2a. In ABAQUS [26], the spring element (SPRING2) is implemented to connect two nodes between core and faceplate. To model spring element behaviour, as shown in Fig. 2b, the constitutive spring contact referred to previous research in [8]. The stiffness of spring contact when in tension is set to zero ($k=0Nm^{-1}$) and is assigned to a high value ($k=210x109Nm^{-1}$) when in compression.

RESULT AND DISCUSSION

Convergence analysis

The mesh convergence in the existing ramp door model was analyzed. The convergence analysis was carried out by using static finite element analysis to get the relation between static response and mesh size, as illustrated in Fig. 3. The method of establishing mesh convergence requires a curve of a critical parameter of von Mises stress and displacement to be plotted against the number of elements. Mesh sizes between 0.1 m and 0.03 m were investigated to obtain accurate mesh sizes. The mesh element size 0.05 m with the number of elements and nodes 210,861 and 279,157, respectively, is chosen as a reliable result.

Result of structural strength analysis

In this section, the finite element results are presented to thoroughly observe the comparison of structural strength between the existing ramp door and modified models. All input of geometry, boundary condition, and the material property is similar to convergence analysis. Fig. 4a pres-

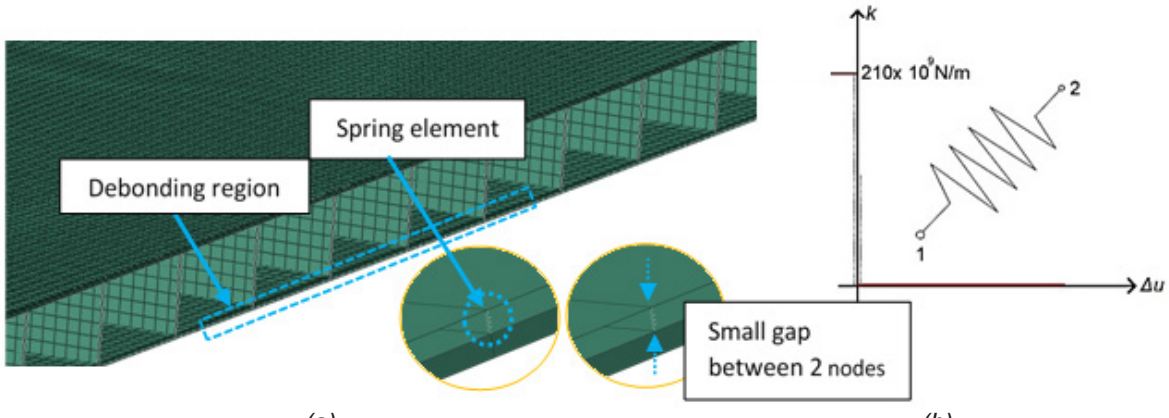

Figure 2: (a) Debonding modelling with spring element (b) the law of spring element contact

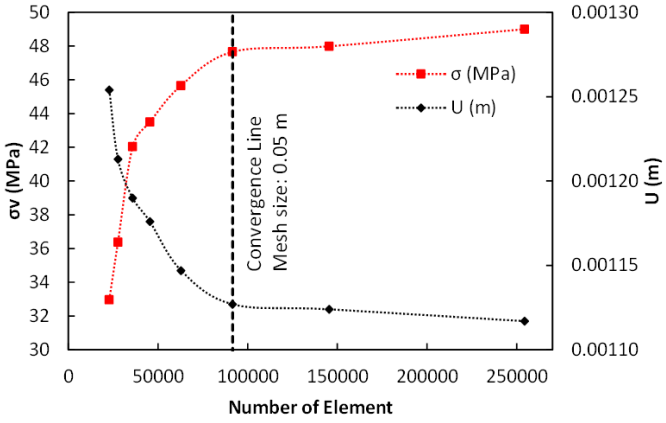

Figure 3: Convergence analysis of the existing model

ents in sequence the comparison between von Mises stress and displacement. From the result, it shows that the application of sandwich panel by reducing the stiffener reduced the von Mises stress and displacement, except in Model E. Comparing between the existing model and Model A which have similar weight, can reduce both von Mises stress up to 32% and displacement up to 35.6%. It can be identified in Fig. 4a that the reduction of stiffener for increasing weight-saving causes an increase in stress and displacement. So, only Model E experiences higher maximum stress and displacement than the existing model.

The reduction of stress and displacement by application of sandwich panel is affected by the difference in thickness configuration and separation of the faceplate by a core material that causes to the significant increase in the sectional modulus and sectional area, which can increase bending stiffness. Optimization of model configuration leads to the searched result, which best fits the optimization target under applied constraints. Fig. 4b presents the strength to weight ratio accumulated from the average stress and weight reduction percentage. The highest strength to weight ratio is concluded to be the optimal model configuration. It can be decided that the new proposed ramp door model configuration is Model C, with a total highest strength to weight ratio of 0.192, as depicted in Fig. 4b. The comparison of von Mises stress contour between the existing model and model A is presented in Fig. 5.

Numerical result of free vibration analysis

Effect of debonding ratio

This section analyzes the effect of the debonding ratio on Model C in the first ten-mode. The ramp door containing a square debonded at the centre with a damage ratio of 2.5%, 5%, 7.5%, and 10% have been analyzed.

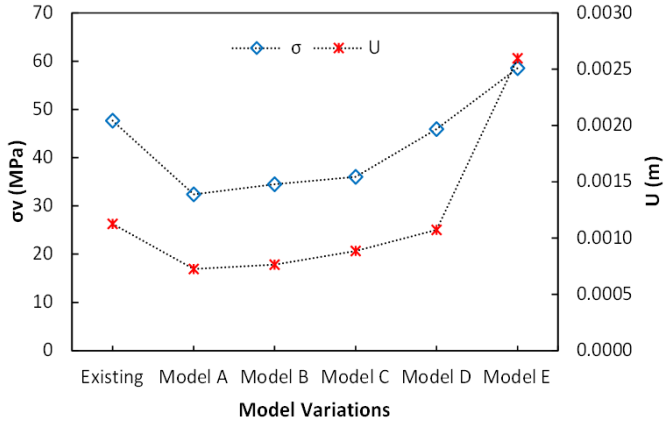

(a)

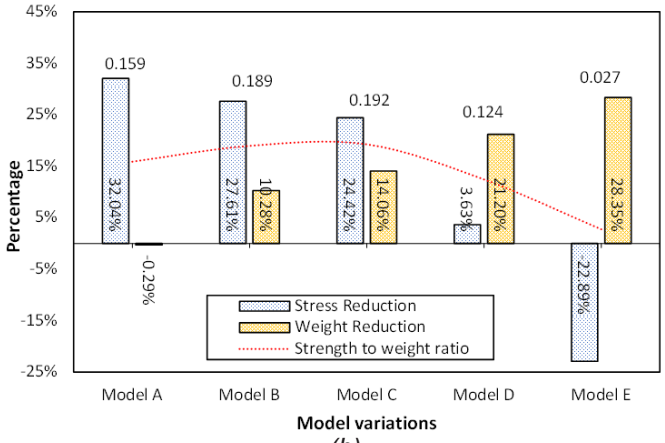

(b)

Figure 4: a) von Mises stress and displacement value b) strength to weight ration and reduction percentage between existing and varied models

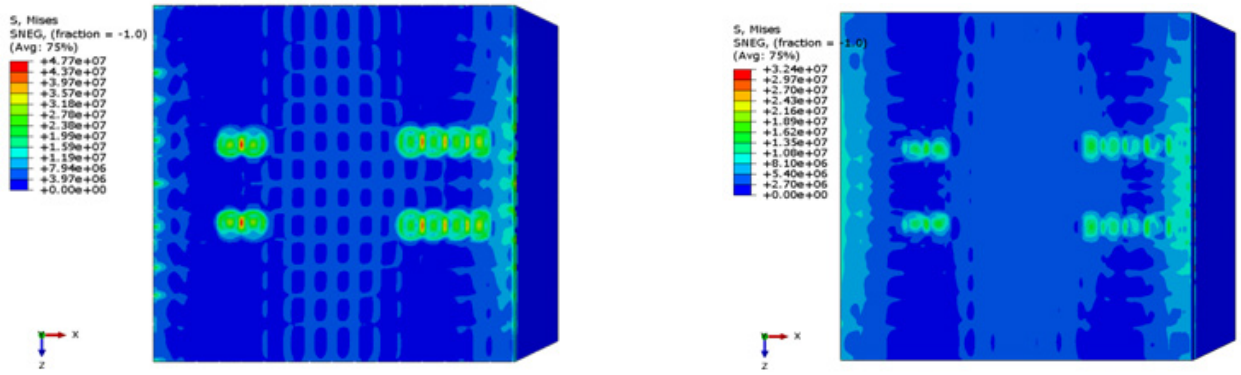

(a) *(b)*

Figure 5: Comparison of von Mises stress contour between a) existing model b) Model A

Both debonding modelling techniques: with spring element and without spring element, have been evaluated. Comparing natural frequencies between the existing and debonded models with two different debonding modellings can be discovered in Fig. 6. Fig. 6a presents the comparison of natural frequency as a function of debonding ratio modelling with the spring contact element. It can be observed that the natural frequencies predominantly decrease with the increase of the debonded ratio, while the first three-mode is practically insensitive. It is noticeable that the frequency changes in the higher modes are more significant than in lower modes. The trend of frequency change is violated due to local thickening phenomenon caused by debonding, that for the first mode and second mode in 2.5% debonding ratio have the frequency of the debonded model higher than the initial model.

The frequency changes of the debonded models increase due to a loss in stiffness and strength of the model, and the mode shapes contain local deformation in the discontinuity area [9]. Besides, it obviously can also be seen that the debonding presence (D% < 5%) does not almost change the lower natural frequencies, only decreases the higher natural frequencies. Another research also noticed this phenomenon in [15]. It can also be seen that the natural frequency changes do not exhibit a monotonous trend as the mode number increases. Hence, it can be summarised that the debonding can influence natural frequencies and is mode dependent.

To obtain more insight, the model without spring contact is also reviewed in Fig. 6b. Debonding causes a high natural frequency change even in the lower mode. Compared with debonding modelling with spring elements, the frequency change in the model without spring contact modelling is more significant in all evaluated modes. Removing the contact might cause inaccurate results, which significantly overestimates the result. Thereby, using the spring contact model, the calculated responses of the debonded model are dampened because contact elements are used to prevent the detached models from overlapping each other. Therefore, the model of the spring contact element is necessary to accurately represent the dynamic response of the debonded model [27].

Effect of debonding geometry

Comparative assessment of the modal characteristics of the ramp door model to the debonding geometry is further examined. Four types of debonding geometry corresponding to the case of interfacial damage such as cir-

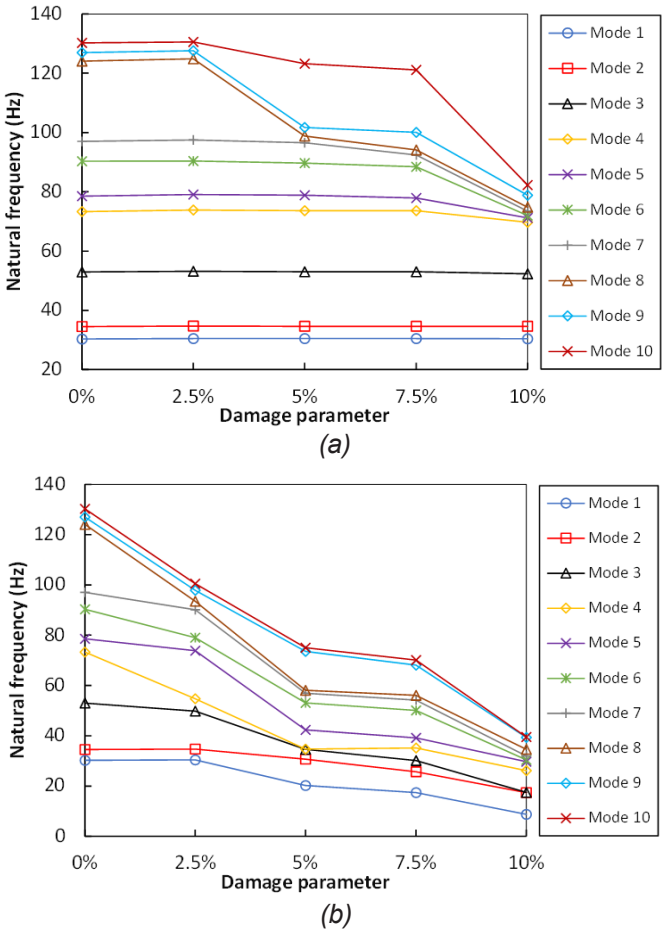

Figure 6: Comparison of natural frequencies as a function of damage parameter between a) with spring element contact b) without spring element contact

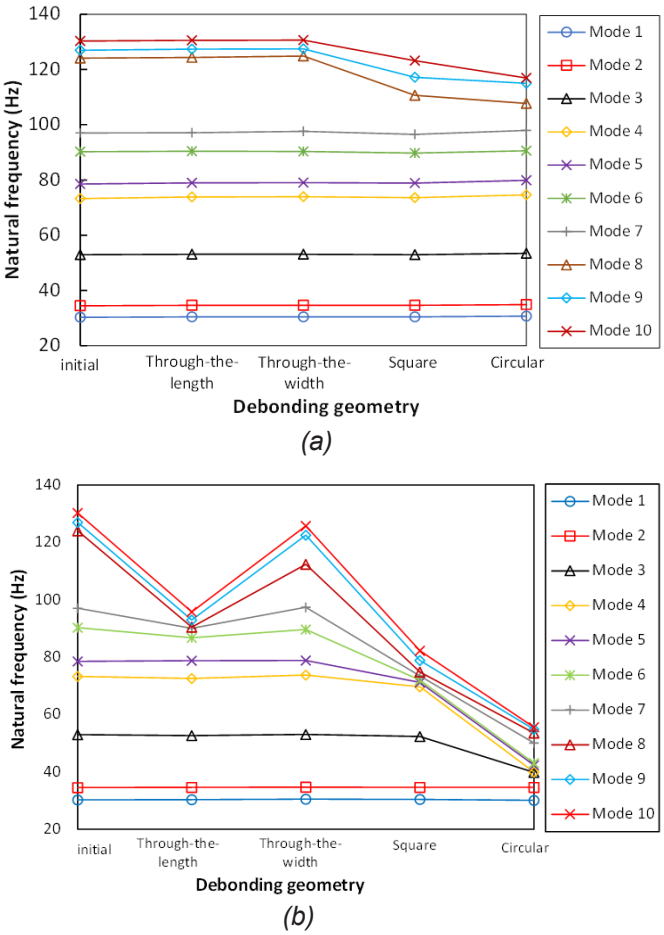

Figure 7: Comparison of natural frequencies as a function of debonding geometry a) 5% debonding ratio b) 10% debonding ratio

cular, square, through-the-length, and through-the-width, were previously investigated in [9]. Debonding geometry was wholly illustrated in [9]. In a previous analysis [9], the effect of debonding geometry was only analyzed in 5% debonding ratio. Hence, further study needs to be conducted using various damage ratio. In this section, the effect of the equally sized debonding geometry was evaluated by both 5% and 10% debonding ratio. All the model discretization is similar to the model in Section 3.3.1.

The comparison of natural frequencies as a function of debonding geometry with two different debonding ratios is depicted in Fig. 7. As observed in Fig. 7a, interfacial debonding induces a decrease in natural frequency, especially in the square and circular debonding geometries. In contrast, there is no significant natural frequency decrease in the through-the-length, and through-the-width debonding geometry. In the lower mode, the natural frequency is altered by small damage but not as significant as in higher modes. Several researchers also mention that debonding detection in the sandwich structure in small damage is more sensitive in higher modes [8, 9, 16, 19]. Debonding decreases the shear stress transfer area between the faceplate and core, which can reduce the stiffness of the model.

Effect of number of debonding

In this section, the influence of the number of debonding on the modal parameters in the first ten-mode is discussed. The model discretization is similar to Section 3.3.1. The comparison of natural frequency between single debonding and multiple debonding with the same damage ratio has been compared. Firstly, circle debonding was modelled as a single debonding with 10% damage ratio. Secondly, debonding was modelled by two and three equally sized circulars debonding. The damage inflicted by these two and three circular debonding zones has equally 10% damage ratio. Models of two and three debonding zones were symmetrically located in the longitudinal midline of the model. As seen in Fig. 8, the frequencies are more affected by the single debonding than the two and three equally sized debonding zones with the same debonding ratio. A model with a single debonding has lower natural frequency than a model with multiple debonding. It can be analyzed that the higher the mode number increased, the more the frequency change increased. However, there is no significant frequency change in lower mode, as shown in mode number 1 and mode number 2, as depicted in Fig. 8. The natural frequencies are the most affected by debonding zones located along the longitudinal midline of the sandwich plate, as also stated in [16]. Further research is needed to be addressed with various debonding ratio and location. As mentioned in [16], using only the natural frequency as a damage parameter is impossible to foresee the location of multiple debonding. To overcome this issue, the associated mode shapes can provide more reliable information. By contour changes in the mode shapes, multiple debonding can be detected.

Effect of debonding depth

To study the influence of debonding depth on the free vibration response, three circulars debonding containing different debonding depth will be analyzed. The damage was modelled by circular debonding located in the bottom sandwich panel with 10% damage ratio. The model discretization is similar to Section 3.3.1. Debonding depth was modelled by creating a gap in the interface layers. The small gap was modelled by creating 10% of core thickness, 20% of core thickness, and 30% of core thickness. The finite element predictions for the first ten-modes associated with various debonding depth are compared in Fig. 9. It can be recognized from Fig. 9 that increasing debonding depth will decrease the natural frequency. Compared with the initial model, the effect of debonding becomes more visible with the increase in the debonding depth. One can see that the model with debonding depth 30% core thickness has the lowest natural frequency compared to other models. Moreover, the frequency changes more rapidly as the mode number increases while the first bending mode practically has no significant effect on the debonding presence. The fre-

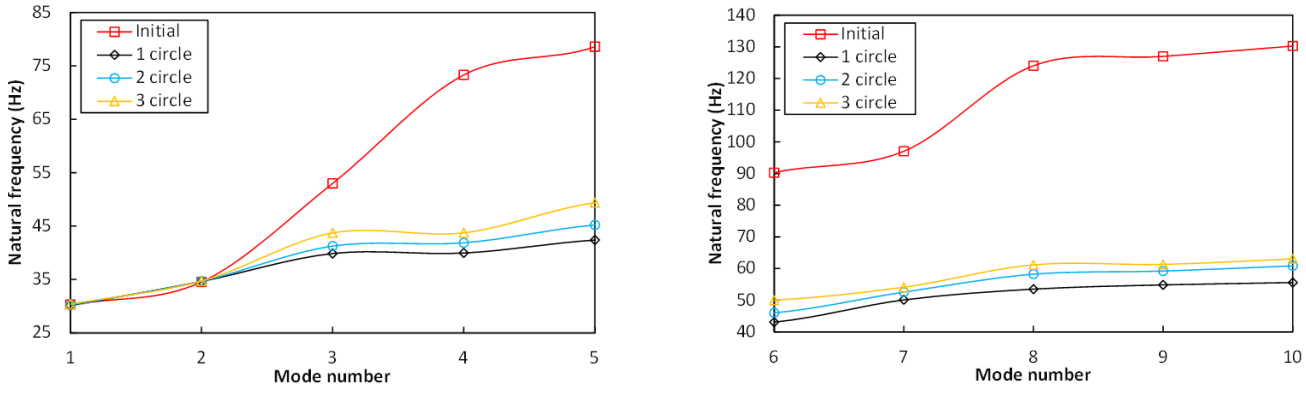

(a) (b)

Figure 8: Natural frequencies of intact and debonding models with different number of debonding (a) mode number 1-5 (b) mode number 6-10

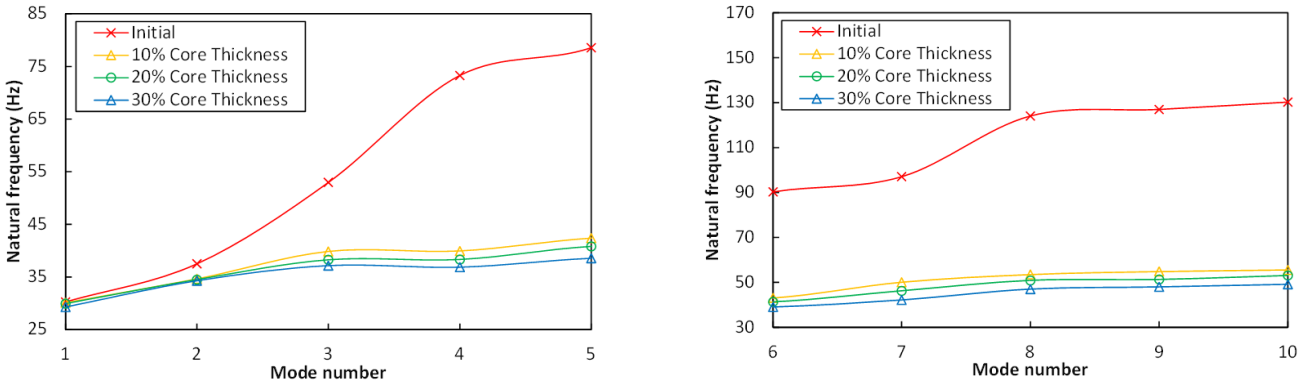

Figure 9: Natural frequencies of intact and debonding models with different debonding depth (a) mode number 1-5 (b) mode number 6-10

quency change of the debonded model increases due to a loss in stiffness caused by initial debonding, and the mode shapes cause a local deformation in the debonded area.

Effect of boundary condition

The effect of boundary condition on the free oscillation behaviour of the damaged ramp door model is researched by analyzing the natural frequency shift. Total of four different boundary conditions reflecting loading condition that may occur on the ramp door was analyzed. They were CCCC (clamped in all side), CFFF (clamped in the rear side, free in other sides), CFCF (clamped in front and rear side and free in other sides), and SFSF (supported in front and rear side and free in other sides). The damage was modelled by circular debonding located in the bottom sandwich panel with 10% damage ratio. Spring element contact was applied. The model discretization is similar to Section 3.3.1. Fig. 10 displays the comparison of the frequency shift between initial and debonded models with different boundary conditions. The highest natural frequency shift is achieved by fully clamped in all sides (CCCC). This trend remains constant for entire analyzed mode numbers. Other result investigations were also mentioned by [28]. It is well-known that a fully clamped boundary condition in all sides produces higher stiffness compared to others with the same geometry

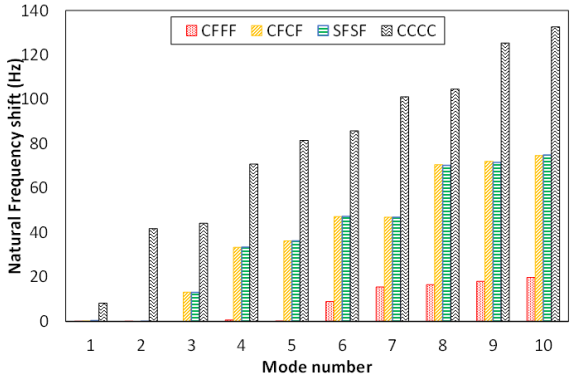

Figure 10: Natural frequencies shift with different boundary conditions

parameters, as also mentioned in [19]. Moreover, the CFCF and SFSF boundary conditions have a similar frequency shift. In contrast, CFFF boundary condition has the lowest natural frequency shift. Further study needs to be handled to obtain the influence of different boundary conditions analyzed on various debonding ratio. Thereby, the debonding corresponding to boundary conditions can be diagnosed by creating damage ratio (D% > 5%), as recommended in [15].

Effect of debonding location

In the final part, the effect of debonding location with the same debonding geometry and ratio has been evaluat-

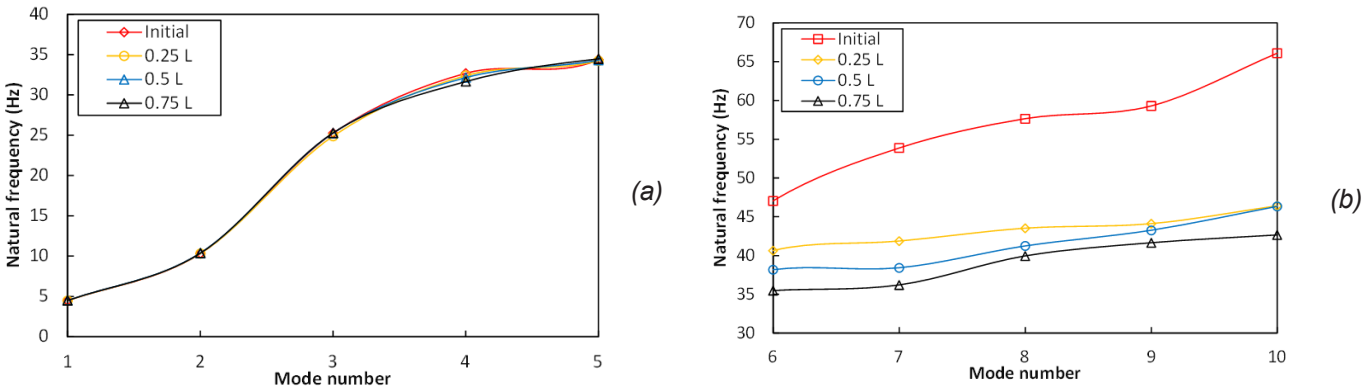

Figure 11: Natural frequencies of intact and debonding models with different debonding location a) mode number 1-5 b) mode number 6-10

ed. Debonding was modelled by circular debonding located in the bottom sandwich panel with 10% damage ratio. Spring element contact was applied in the debonding area with clamped in the rear side and free on the other sides boundary condition (CFFF) was applied. All the model discretization is similar to Section 3.3.1. The variation of three different debonding locations is 0.25L (closest to the clamped edge), 0.5L (in the middle of the structure), and 0.75L (far away from the clamped edge).

As can be seen in Fig. 11, it can be assumed that the effect of debonding with different damage locations can be seen in high mode. In contrast, there is no significant frequency change in the low mode, particularly in mode 1 until mode 5. The farther the location of the damage from the clamped edge, the higher the natural frequency change. It is caused by the lowest stiffness of the front ramp door because of removing the stiffener, which can cause local deformation. Thus, the natural frequency can be used as a parameter to detect debonding location on the ramp door model.

CONCLUSION

In summary, the primary observations and obtained result due to the application of sandwich panel on the ferry ro-ro ramp door on static and dynamic characteristic using finite element software ABAQUS was presented. Firstly, the preliminary study indicates promising results in terms of structural strength and weight saving. Its application contributes to the increase in strength to weight ratio of about 20.75% in Model C. Secondly, the influence of the face sheet-core debonding on the modal characteristics of the damaged ramp door is studied by comparing natural frequency both for intact and debonded models. It is found that higher natural frequency is more sensitive. Thirdly, the sensitivity of natural frequencies is affected by debonding ratio, debonding geometry, number of debonding, debonding depth, debonding location, boundary condition of the models. Thus, using a change resulting from the comparison of the modal parameter, the debonding diagnostics over a wide range of debonding parameters can be performed.

Although several studies on the dynamic characteristic of the debonded sandwich are widely reported in the literature, numerical analysis of vibration-based damage detection on ship structure with various debonding parameter analyzed using general dynamic analysis with nonlinear debonding contact modelling further need to be investigated.

ACKNOWLEDGEMENT

The research leading to these results has received financial support from the Master towards Doctoral Education Program for Excellent Graduate (PMDSU) of the Ministry of Research, Technology and Higher Education of The Republic of Indonesia with contract number 3/AMD/E1/KP.PTNBH/2020.

REFERENCES

1. Yang, J.S., Ma, L., Schmidt, R., Qi, G., Schröder K.U., Xiong, J., Wu, L.Z. (2016). Hybrid lightweight composite pyramidal truss sandwich panels with high damping and stiffness efficiency. Composite Structures, vol. 148, 85–96, DOI: 10.1016/j.compstruct.2016.03.056
2. Sujiatanti, S.H., Zubaydi, A., Budipriyanto, A. (2018). Finite Element Analysis of Ship Deck Sandwich Panel. Applied Mechanics and Materials, vol. 874, 134-139, DOI: 10.4028/www.scientific.net/AMM.874.134
3. Tuswan, Abdullah, K., Zubaydi, A., Budipriyanto, A. (2019). Finite-element Analysis for Structural Strength Assessment of Marine Sandwich Material on Ship Side-shell Structure. Materials Today: Proceedings, vol. 13, no. 1, 109–11, DOI: 10.1016/j.matpr.2019.03.197
4. Ramakrishnan, K.V., Kumar D.P.G. (2016). Applications of Sandwich Plate System for Ship Structures. IOSR Journal of Mechanical and Civil Engineering (IOSR-JMCE), 83-90.
5. Mamalis, A. G., Spentzas, K. N., Pantelelis, N. G., Manolakos, D. E., Ioannidis, M. B. (2008). A new hybrid concept for sandwich structures. Composite Structures, vol. 83, no. 4, 335–340, DOI: 10.1016/j.compstruct.2007.05.002
6. Savin-Barcan, M., Beznea, E.F., Chirica, I. (2018). Influence of fabrication imperfections on dynamic response of a sandwich composite panel of a ship deck structure. IOP Conference Series: Materials Science and Engineering, vol. 400, 1-6, DOI:10.1088/1757-899X/400/3/032008
7. Tuswan, Zubaydi, A., Budipriyanto, A., Sujiatanti, S.H. (2018). Comparative study on ferry ro-ro's car deck structural strength by means of application of sandwich materials. Proceedings of the 3rd International Conference on Marine Technology (SENTA), vol. 1, p. 87-96.
8. Tuswan, Zubaydi, A., Piscesa, B., Ismail, A. (2020). Dynamic characteristic of partially debonded sandwich of ferry ro-ro's car deck: a numerical modelling. Open Engineering, vol. 10, 424-433, DOI: 10.1515/eng-2020-0051
9. Tuswan, Zubaydi, A., Piscesa, B., Ismail, A., Ilham, M.F. (2020). Free vibration analysis of interfacial debonded sandwich of ferry ro-ro's stern ramp door. Procedia Structural Integrity, vol. 27C, 22-29. DOI: 10.1016/j.prostr.2020.07.004
10. Birman, V., Kardomateas, G.A. (2018). Review of current trends in research and applications of sandwich structures. Composites Part B: Engineering, vol. 142, 221-240, DOI: 10.1016/j.compositesb.2018.01.027

11. Burlayenko, V.N., Sadowski, T. (2018). Linear and Nonlinear Dynamic Analyses of Sandwich Panels with Face Sheet-to-Core Debonding. Shock and Vibration, vol. 2018, 1-26, DOI: 10.1155/2018/5715863
12. Bragagnolo, G., Crocombe, A.D., Ogin, S.L., Mohagheghian, I., Sordon, A., Meeks, G., Santoni, C. (2020). Investigation of skin-core debonding in sandwich structures with foam cores. Materials & Design, vol. 186, 1-10, DOI: 10.1016/j.matdes.2019.108312
13. Chen, Y., Hou, S., Fu, K., Han, X., Ye, L., (2017). Low-velocity impact response of composite sandwich structures: modelling and experiment. Composite Structures, vol. 168, 322–334, DOI: 10.1016/j.compstruct.2017.02.064
14. Fatt, M.S.H., Sirivolu, D. (2017). Marine composite sandwich plates under air and water blasts. Marine Structures, vol. 56, 163–185, DOI: 10.1016/j.marstruc.2017.08.004
15. Burlayenko, V.N., Sadowski, T. (2010). Influence of skin/core debonding on free vibration behavior of foam and honeycomb cored sandwich plates. International Journal Non-Linear Mechanics, vol. 45, 959-968, DOI: 10.1016/j.ijnonlinmec.2009.07.002
16. Burlayenko, V.N., Sadowski, T. (2011). Dynamic behaviour of sandwich plates containing single/multiple debonding. Computational Materials Science, vol. 50, 1263–1268, DOI: 10.1016/j.commatsci.2010.08.005
17. Yang, C., Hou, X.B., Wang, L., Zhang, X.H. (2016). Applications of different criteria in structural damage identification based on natural frequency and static displacement. Science China Technological Sciences, vol. 59, 1746–1758, DOI: 10.1007/s11431-016-6053-y
18. Zhao, B., Xu, Z., Kan, X., Zhong, J., Guo, T. (2016). Structural damage detection by using single natural frequency and the corresponding mode shape. Shock and Vibration, vol. 2016, 1-8, DOI: 10.1155/2016/8194549
19. Ismail, A., Zubaydi, A., Piscesa, B., Ariesta, R.C., Tuswan. (2020). Vibration-based damage identification for ship sandwich plate using finite element method. Open Engineering, vol. 10, 744 – 752, DOI: 10.1515/eng-2020-0086
20. Kaveh, A., Zolghadr, A. (2015). An improved CSS for damage detection of truss structures using changes in natural frequencies and mode shapes. Advances in Engineering Software, vol. 80, 93-100, DOI: 10.1016/j.advengsoft.2014.09.010
21. Elshafey, A.A., Marzouk, H., Haddara, M.R. (2011). Experimental damage identification using modified mode shape difference. Journal of Marine Science and Application, vol. 10, 150–155, DOI: 10.1007/s11804-011-1054-5
22. Zhu, K., Chen, M., Lu, Q., Wang, B., Fang, D. (2014). Debonding detection of honeycomb sandwich structures using frequency response functions. Journal of Sound and Vibration, vol. 333, no. 21, 5299–5311, DOI: 10.1016/j.jsv.2014.05.023
23. Burlayenko, V.N., Sadowski, T. (2014). Nonlinear dynamic analysis of harmonically excited debonded sandwich plates using finite element modelling. Composite Structures, vol. 108, 354-366, DOI: 10.1016/j.compstruct.2013.09.042
24. DNV-GL. Steel sandwich panel construction, from www.dnvgl.com/rules-standards, accessed on 2020-05-05.
25. DNV-GL. Rules for Classification High Speed and Light Craft, from www.dnvgl.com/rules-standards, accessed on 2020-05-06.
26. Dassault Systemes Simulia Corp. Abaqus Analysis User Guide, from: http://ivt-abaqusdoc.ivt.ntnu.no:2080/v6.14/books/usb/default.html, accessed on 2020-05-07.
27. Burlayenko, V.N., Sadowski, T. (2011). Numerical Modelling of Sandwich Plates with Partially Dedonded Skin-to-Core Interface for Damage Detection, The 8th International Conference on Structural Dynamics, p. 1-8.
28. Lou, J., Wu, L., Ma, L., Xiong, J., Wang, B. (2014). Effects of local damage on vibration characteristics of composite pyramidal truss core sandwich structure. Composites Part B: Engineering, vol. 62, 73–87, DOI: 10.1016/j.compositesb.2014.02.012

Paper submitted: 29.07.2020.
Paper accepted: 13.10.2020.